I&EC research
Industrial & Engineering Chemistry Research

Article

pubs.acs.org/IECR

Online Optimal Feedback Control of Polymerization Reactors: Application to Polymerization of Acrylamide−Water−Potassium Persulfate (KPS) System

Navid Ghadipasha,[†] Wenbo Zhu,[†] Jose A. Romagnoli,*[,†] Terry McAfee,[‡] Thomas Zekoski,[‡] and Wayne F. Reed[‡]

[†]Department of Chemical Engineering, Louisiana State University, Baton Rouge, Louisiana 70803, United States
[‡]Department of Physics and Engineering Physics, Tulane University, New Orleans, Louisiana 70118, United States

ABSTRACT: This paper deals with the design and implementation of optimal real-time control strategies for controlling polymerization reactors in free radical polymerization processes. A multiobjective optimization problem is first formulated to determine optimal trajectories for a range of target products. A tailor-made control module is then formulated and implemented in python for controlling the weight-average molar mass (M_w) to robustly achieve the desired polymer molar mass distribution (MMD). Multiple control case studies are discussed and applied to force the system along the optimal targets. Performance of the controller is evaluated in each case using Automatic Continuous Online Monitoring of Polymerization reactions (ACOMP). Results are provided through investigations into the free radical polymerization of the acrylamide in water using potassium persulfate (KPS) as an initiator.

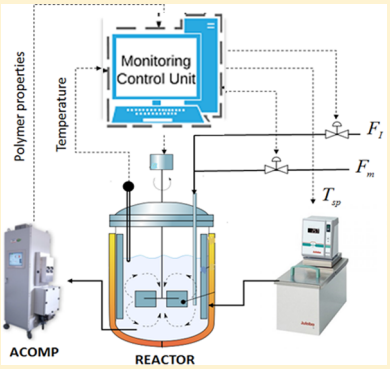

1. INTRODUCTION

Control of polymerization reactors is an important section of the chemical industry which enables mass production of polymers with reliable quality. Producing uniform and specific polymers is of paramount importance to end user manufacturers who need their products to be consistent for specific applications. Although advanced full feedback control of many types of reactors has been available for many years,[1,2] the technology is less advanced for the polymeric systems. The principal difficulty in controlling polymerization reactors is related to inadequate real-time measurement techniques which can provide consistent online data along a polymerization reaction. Many of the process variables which affect the quality of polymers such as polymer molar mass averages are difficult to measure online, or they can be measured only at low sampling frequencies with long time delays which are inadequate for monitoring and control purposes. Polymerization reactions are also highly sensitive and have complex dynamics due to nonlinearities arising during the reaction because of gelation, high exothermicity, and severe changes in kinetic coefficients of the system (e.g., propagation and termination rate).[3] This makes product quality achievement a much more complex issue and necessitates development of a proper control strategy to regulate polymerization systems.

A primary goal in most of the polymerization reactions is to synthesize polymers with specific molar mass distribution (MMD). This is a fundamental polymer property which can markedly affect the physical, rheological, and thermal properties of polymers such as strength, processability, and thermal stability.[4−8] Because of the sensitive molecular structure of polymers, MMD can change owing to many factors such as concentration of materials, reactor temperature, or degree of mixing.[9] The main problem in controlling MMD is the lack of reliable techniques in monitoring molar mass distributions and the molar mass averages such as number-average (M_n) and weight-average molar mass (M_w). This is a necessity for feedback control of MMD.

Because of the aforementioned issues, most of the control works in the literature have been either open-loop or focused on controlling other parameters such as reactor temperature and density, which are indirectly related to the molar mass averages and MMD. Recent developments in polymerization reactor control have been critically reviewed by Yoon et al. and Kreft et al.[10,11] One approach that was routinely used was predetermining the desired manipulated variable trajectories. In this case, the trajectory of the manipulated variable is generated by some means, and it is assumed that by tracking the selected trajectory, the control variable can achieve the desired target. For example, Crowley and Choi et al.[12−14] introduced a method for optimal control of chain length distribution in a batch free radical polymerization. They managed to follow the desired chain length distribution by manipulating the temperature profile inside the reactor. A sequence of discrete reactor temperature set-points which lead to the desired chain length distribution were computed using an optimization program on the basis of sequential quadratic programming. Then, an online execution level controller

Received: March 14, 2017
Revised: May 26, 2017
Accepted: June 1, 2017
Published: June 1, 2017

DOI: 10.1021/acs.iecr.7b01074
Ind. Eng. Chem. Res. 2017, 56, 7322−7335

was applied to track the optimal temperature profile by manipulating the coolant flow, fed to the reactor jacket. Similarly, Chang and Liao et al.[15] applied a modified two-step method in calculating the optimal temperature trajectory in order to obtain a prescribed MMD. First, the profiles of the instantaneous average chain length for a desired MMD were estimated, and the time profile of the reactor temperature was obtained on the basis of the instantaneous average chain length trajectory. Next, a conventional PI controller with suitable tuned parameters was applied to track the optimal temperature recipe. Both these methods heavily depend on an accurate model to predict the optimal trajectories for the manipulated variable. To consider the model inaccuracy, Kiparissides et al.[16] proposed an online estimator-optimization scheme to update the optimal control policy at each iteration and provide reliable estimates for process parameters to account for the impact of model parameter variations on online control of the system. In the final layer of their framework, the time optimal sequence of temperature set-point changes is passed to a regulatory controller to force the process to follow the optimal trajectory as close as possible. Results showed good agreement with the desired polymer product quality for batch systems. However, the absence of the feedback control on the control variable makes this technique vulnerable to plant disturbances such as temperature or flow variations.

There has also been a significant amount of work using model predictive control (MPC) in the area of polymerization reactors. For example, Alhamad et al.[17] developed a multilayer control algorithm for real-time implementation of optimal control policies on emulsion copolymerization. A multi-input−multi-output (MIMO) formulation was constructed to maximize the M_n and M_w. Due to lack of online sensor in predicting MMD, a "soft-sensor approach" was applied using the dynamic models to provide an online estimate of the MMD and M_w. Park and Rhee[18] also used a nonlinear model in the learning algorithm of the MPC and investigated the effectiveness of the proposed nonlinear predictive controller (NMPC) in the case of semibatch solution copolymerization of methyl methacrylate/methyl acrylate. For online measurement of M_w, a correlation was used by measuring the specific viscosity η_{sp} and solving the Mark−Houwink equation to calculate M_w.[19] Other contributions also suggested use of NMPC for control of nonlinear systems.[20,21] However, robust closed-loop control methods involving direct online measurement of the process output variable would have to be developed for better control.

Over the past 20 years, Automatic Continuous Online Monitoring of Polymerization processes (ACOMP) has been developed and studied by Reed and Alb.[22] ACOMP, which is a widely applicable platform for monitoring polymerization reactions, relies on continuous extraction and dilution of small sample streams from the reactor on which the analyses are made by different combinations of detectors such as light scattering, UV/visible spectrophotometry, viscometry, refractivity, conductivity, and polarimetry. This allows tracking of certain polymer characteristics including monomer conversion and weight-average molar mass. ACOMP can be applied in free radical, controlled free radical, condensation reactions, emulsion, and inverse emulsion polymerization in batch, semibatch, and continuous reactors. Online monitoring of polymerization reactions as they occur paves the way for integration of monitoring, optimization, and feedback control of polymerization processes.

Automatic control of free radical acrylamide polymerization was recently demonstrated using ACOMP and an alternate controller that did not involve a detailed kinetic model.[23] In this contribution, real-time implementation of an optimal controller for controlling M_w and MMD is addressed. An experimentally validated nonlinear process model is used first to perform dynamic optimization studies. A similar approach presented by Crowley and Choi[13] is applied to acquire the complete MMD. This technique which calculates the mass fraction of polymers with different chain lengths based on the kinetic rate equations has been slightly modified so it can deal with semibatch systems. The validated model is then used for model-based optimization to determine the optimal temperature, monomer, and initiator flow rates for a final desired polymer MMD. These optimal profiles are implemented on the experimental reactor system, and the M_w trajectories are compared with the theoretical predictions. Results demonstrate the insufficiency of the open-loop approach due to model inaccuracy and process disturbances. Therefore, results from the dynamic optimization are used as the set point of the controller for the real-time feedback control to maintain the process along the established open-loop optimal state trajectories. A tailor-made control module is formulated and implemented in the Python environment, which is free and open-source software, supporting multiple programming paradigms such as object-oriented and functional programming styles. A number of alternative operating scenarios are validated using the experimental facilities. Polymerization of acrylamide in water using potassium persulfate (KPS) as an initiator is used as an illustrative example to demonstrate the effectiveness of the real-time optimal control environment.

2. OPTIMIZING CONTROL OF POLYMERIZATION SYSTEMS

Process Model. The model equations for free radical polymerization of the acrylamide system are presented in this section, which contains mass and moment balances. The model was tested experimentally using the same approach proposed previously by Ghadipasha et al.[24] Assuming small chain transfer, the system of equations can be written as

$$\frac{dN_m}{dt} = -(k_p + k_{fm})P_0N_m + F_mC_{mf} - F_{out}{}^*C_m \quad (1)$$

$$\frac{dN_i}{dt} = -k_dN_i + F_iC_{if} - F_{out}{}^*C_i \quad (2)$$

$$\frac{dN_s}{dt} = -k_{fs}N_sP_0 + F_iC_{sif} + F_mC_{smf} - F_{out}{}^*C_s \quad (3)$$

$$\frac{d(\lambda_0V)}{dt} = (k_{fm}N_m + k_{td}P_0V + k_{fs}N_s)\alpha P_0 + \frac{1}{2}k_{tc}P_0^2V \quad (4)$$

$$\frac{d(\lambda_1V)}{dt} = [(k_{fm}N_m + k_{td}P_0V + k_{fs}N_s)(2\alpha - \alpha^2) + k_{tc}P_0V]\frac{P_0}{(1-\alpha)} \quad (5)$$

$$\frac{d(\lambda_2V)}{dt} = \left[(k_{fm}N_m + k_{td}P_0V + k_{fs}N_s)(\alpha^3 - 3\alpha^2 + 4\alpha) + k_{tc}P_0V(\alpha+2)\frac{P_0}{(1-\alpha)}\right]\frac{P_0}{(1-\alpha)^2} \quad (6)$$

DOI: 10.1021/acs.iecr.7b01074
Ind. Eng. Chem. Res. 2017, 56, 7322−7335

where $N_m = C_m V$, $N_i = C_i V$, $N_s = C_s V$, and

$$\alpha = \frac{k_p C_m}{k_p C_m + k_{fm} C_m + k_{fs} C_s + k_{tc} P_0 + k_{td} P_0} \quad (7)$$

$$P_0 = \sqrt{\frac{2fC_i k_d}{k_t}} \quad (8)$$

$$V = \left[1 - \frac{\lambda_1 w_m}{\rho_p}\right]^{-1} \left[\frac{N_m w_m}{\rho_m} + \frac{N_s w_s}{\rho_s} + \frac{N_i w_i}{\rho_i}\right] \quad (9)$$

$$\rho_s = -0031(T^2) - 0.1437T + 1003 \quad (10)$$

Monomer conversion:

$$X = \frac{N_{m0} + \int_0^t F_m C_{mf}\, dt - C_m V - \int_0^t F_{out} {}^* C_m\, dt}{N_{m0} + \int_0^t F_m C_{mf}\, dt} \quad (11)$$

Number-average and weight-average molar mass:

$$M_n = w_m \frac{\lambda_1}{\lambda_0},\ M_w = w_m \frac{\lambda_2}{\lambda_1} \quad (12)$$

Chain length distribution:

$$\frac{df(m,n)}{dt} = \frac{1}{\lambda_1} k_p C_m \left(\left[\frac{m(1-\alpha)+\alpha}{\alpha}\right] \alpha^{m-1} - \left[\frac{(n+1)(1-\alpha)+\alpha}{\alpha}\right] \alpha^n \right) P - \frac{1}{\lambda_1 V} f(m,n) \frac{d(\lambda_1 V)}{dt} \quad (13)$$

Here, N_m, N_i, and N_s represent the total moles of monomer, initiator, and solvent inside the reactor. V is the volume of the content of the reactor, and F_m and F_i are the flow rates of the monomer and initiator, which are fed to the reactor in the semi-batch mode. Eqs 4−6 describe the dynamic of the corresponding moments (λ_0, λ_1, and λ_2) for the dead polymers. A complete description of all the variables is available in the notation section. System properties such as densities and heat capacities were obtained from the literature, while the values of the kinetic rate constants were estimated from experimental data using a parameter estimation analysis as demonstrated by Ghadipasha et al.[24] It is assumed that the kinetic rate constants follow an Arrhenius type equation:

$$k = A e^{-E_a/(RT)} \quad (14)$$

Estimated values of the kinetic rate constants as well as the thermodynamic parameters for the acrylamide system are displayed in Table 1.

The system of equations, describing the dynamic of M_w, M_n, and chain length distribution fractions are valid when the concentration of live polymer in the system is negligible, which is the case when the polymerization system is either dilute (in solution polymerization) or the conversion of the monomer is not very high (in bulk polymerization). In this work, the Am is polymerized up to high conversion, but the reactor content is always kept dilute at a solids level that is safe and controllable with respect to temperature. The proposed model is used next for optimization and control purposes.

Table 1. Kinetic and Thermodynamic Parameters of the Dynamic Model

parameter	explanation	value	unit
A_d	pre-exponential factor for decomposition rate constant	7.15×10^{12}	[1/min]
E_d	activation energy for decomposition rate constant	−101 123.182	[J/mol]
A_p	pre-exponential factor for propagation rate constant	4.08×10^5	[m³/mol·min]
E_p	activation energy for propagation rate constant	−11 700	[J/mol]
A_t	pre-exponential factor for termination rate constant	4.08×10^9	[m³/mol·min]
E_t	activation energy for termination rate constant	−11700	[J/mol]
ρ_m	monomer density	1130	[kg/m³]
ρ_p	polymer density	1302	[kg/m³]
ρ_s	solvent density	eq 10	[kg/m³]
ρ_i	initiator density	2480	[kg/m³]
f	initiator efficiency factor	0.196	

Free Radica Polymerization Kinetics and Weight-Average Molar Mass (M_w) Calculation. Controlling M_w has a high impact on the final distribution of polymers. Thus, it is of interest to investigate the effect of different parameters on M_w as well as determine a formulation which can lead to a certain M_w trajectory and final MMD target. Assuming small chain transfer to the monomer and solvent, the instantaneous number average of a polymer which is produced at time t is given by

$$N_{n,inst} = \frac{k_p[C_m]}{Y k_t[P_0]} \quad (15)$$

where Y is a factor which is equal to 1 when the termination reaction is dominated by recombination and 2 when disproportionation dominates. The cumulative weight-average molar mass $M_w(t)$ can then be obtained by knowing the mass of dead polymers inside the reactor, $m_p(t)$, as follows:

$$M_w(t) = \frac{\int_0^t w M_m N_{n,inst} dm_p(t)}{m_p(t)} \quad (16)$$

Here, w and M_w are the instantaneous polydispersity and the monomer molecular weight, respectively. Assuming constant temperature, which results in constant kinetic rate parameters, the only two terms which vary during the reaction are the concentration of the monomer $[C_m]$ and live radicals $[P_0]$, both of which can be manipulated using the monomer and initiator flows. This gives the opportunity to propose various trajectories of M_w by proper formulation of the optimization problems.

Dynamic Optimization. Offline model-based optimization of the process is explained in this part. There are several benefits regarding optimization of the system. First, multiple control objectives can be considered simultaneously. Furthermore, constraints on the process and control variables can be dealt with explicitly in the formulation of the optimization. gOPT, an optimization facility in gPROMS, was used to perform the optimization in this work. The selection of this tool is motivated primarily by the fact that the model simulation solution is performed in the gPROMS environment. Second, the gOPT code employs piecewise control variable definition, which is convenient for real-time implementation. Decision variables in this case vary according to a piecewise constant function, indicating that they have a constant value for a certain amount of

DOI: 10.1021/acs.iecr.7b01074
Ind. Eng. Chem. Res. 2017, 56, 7322−7335

time depending on the interval, and then they change to another value for the next interval.[24] The optimizer applies the "single-shooting" method in order to find the optimal solution of the system, which can be explained in four steps. First, the optimizer selects the time intervals for the different decision variables such as monomer and initiator flow with their corresponding values over each interval. Next, knowing the initial condition of the system, the set of equations can be solved to find the solution for the different state variables. The values of the objective function as well as the process constraints are then evaluated, and based on their values the optimizer revises the choices and repeats this procedure until it converges to an optimal solution. A complete explanation of this approach can be found in Schlegel et al.[25] (dynamic optimization using adaptive control vector parametrization). In the following, an optimization study for a number of operational scenarios with different M_w trajectories is illustrated. The temperature is assumed to be constant at the optimal value during the reaction, while the monomer and initiator flows can change at different time intervals. It is important to keep the reactor isothermal along the whole process as temperature fluctuations can significantly influence the M_w behavior. The temperature change can be considerable at high polymer concentration due to an increase in the viscosity of the solution which causes heat transfer issues between the reaction medium and the tube walls.

Case 1: Decreasing Trajectory of M_w. This is the most common trend of M_w in polymerization reactions which naturally occurs in free radical batch polymerization. At the beginning of the process when the monomer concentration is high, polymers with long chain lengths are formed, resulting in high M_w. Gradually, by depletion of the monomer in the reactor, the length of the produced polymer reduces, resulting in smaller M_w. By proper formulation of the optimization problem, it is possible to obtain a certain decreasing trajectory with a specific final value for M_w. The expression for the objective function in this case is shown as follows:

$$J = w_1\left(\frac{X_f}{X_t} - 1\right)^2 + w_2\left(\frac{M_{w,f}}{M_{w,t}} - 1\right)^2 + w_3\sum_{nc}^{i=1}\left(\frac{f_{i,f}}{f_{i,t}} - 1\right)^2 + w_4(N_{mf,f}) \quad (17)$$

where the index f is used to represent the final value for the optimization variable and t stands for the final target. w_i's are the coefficients, determining the importance of each term in the objective function. Parameter values for the objective functions are presented in Table 2. The $f_{i,t}$'s are the target values for the chain length fraction in the probability function at each chain length interval. The number of $f_{i,t}$'s is selected such that the weight fraction of the polymer bounded by the chain lengths is 99.9% of the total polymer produced at final monomer conversion. Values for $f_{i,t}$'s are reported in Table 5, Appendix A for each optimization scenario.

A summary of the initial loading and different constraints of the reactor is shown in Table 3. F_{min} and F_{max} are the ranges in which the pump can operate while V_{min} and V_{max} are the volume constraints to ensure the reactor volume will not exceed the maximum reactor capacity. Figure 1 depicts the time optimal temperature, monomer, and initiator flow profiles. As it is presented in the flow profiles, at the beginning of the reaction the flow rate of monomer to the reactor is high, while the initiator feed is rather low. However, in order to reduce M_w, the optimizer decreases the monomer flow after some time, while increasing the initiator feed to keep the free radical concentration high. This will reduce the instantaneous number-average of the polymers, and as a result the cumulative weight-average molar mass (M_w) also decreases. Results for the monomer concentration (as an index of conversion) and M_w with their corresponding targets are shown in the lower panel of Figure 1. MMD has also been shown at the final time of the simulation. There is a very good agreement between the simulation results and the corresponding targets. This shows the benefits of combining reagent and monomer flow with temperature as a decision variable in the optimization. Not only the monomer concentration and M_w but also the complete distribution (MMD) can be achieved properly.

Table 2. Parameter Values of the Different Objective Functions

optimization #	description	w_1	w_2	w_3	w_5	X_t	$M_{w,t}$
1	decreasing M_w	0.5	0.25	0.5	1	0.9	650
2	constant M_w	1	0.05	0.5			
3	increasing M_w	0.5	1	0.05		0.75	500

Table 3. Initial Loading and Ranges of Optimization Constraints

operational parameter	value
N_m [mole]	0.3
N_s [mole]	50
N_i [mole]	0.005
F_{max} [mL/min]	5
F_{min} [mL/min]	0.1
T_{max} [°C]	80
T_{min} [°C]	40
V_{max} [mL]	1200
V_{min} [mL]	450

Case 2: Constant M_w. According to eq 15, by keeping a constant ratio between the monomer and free radical concentration, the instantaneous number-average molar mass and, as a result, M_w will stay constant during the reaction. So an attempt was made to reach a constant trajectory of M_w. The objective function in this case is formulated as follows:

$$J = w_1\int_0^{t_f}\left|\frac{\partial M_w}{\partial t}\right|dt + w_2\sum_{nc}^{i=1}\left(\frac{f_{i,f}}{f_{i,t}} - 1\right)^2 + w_3(N_{mf,f}) \quad (18)$$

Monomer conversion was eliminated from the objective function to put more weight on the other terms as it is more demanding in this case to reach a constant M_w profile. The initial loading of the reactor and the constraints are the same as in the previous case. However, the monomer and initiator flows were diluted with solvent to avoid control saturation (later in the control experiment) and sudden change in the control variable. Simulation results are shown in Figure 2. M_w follows a constant trajectory, and there is a good match between the final distribution results and the targets. From the manipulated variable profiles, it can be deduced that while the optimizer almost keeps a constant flow rate of monomer, it gradually reduces the initiator flow to compensate for monomer consumption and keep the ratio between the monomer and free radicals constant. It must be mentioned that in this case the values of the monomer and initiator flows change at each time interval (2.5 min) as opposed to the previous case where they

DOI: 10.1021/acs.iecr.7b01074
Ind. Eng. Chem. Res. 2017, 56, 7322−7335

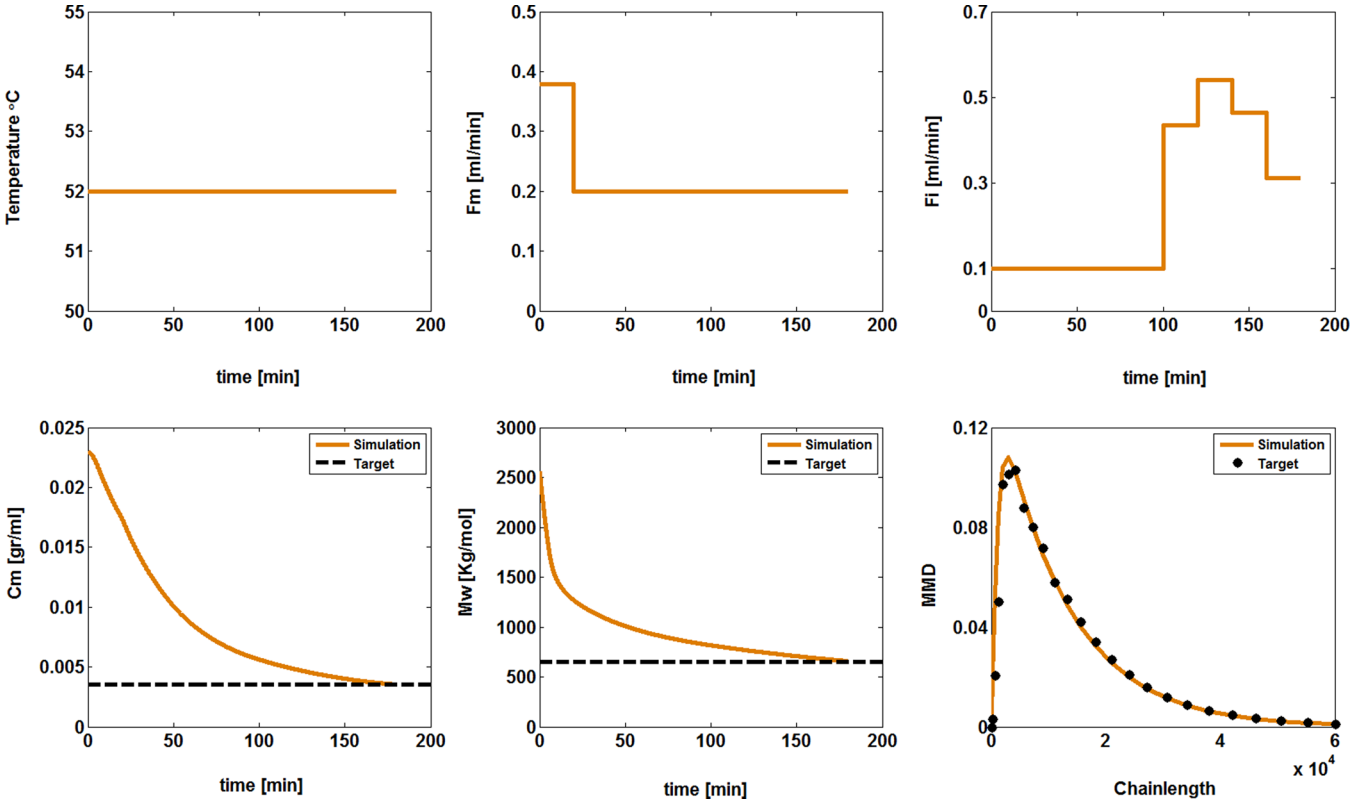

Figure 1. Simulation results applying the optimal trajectories for the decreasing M_w scenario.

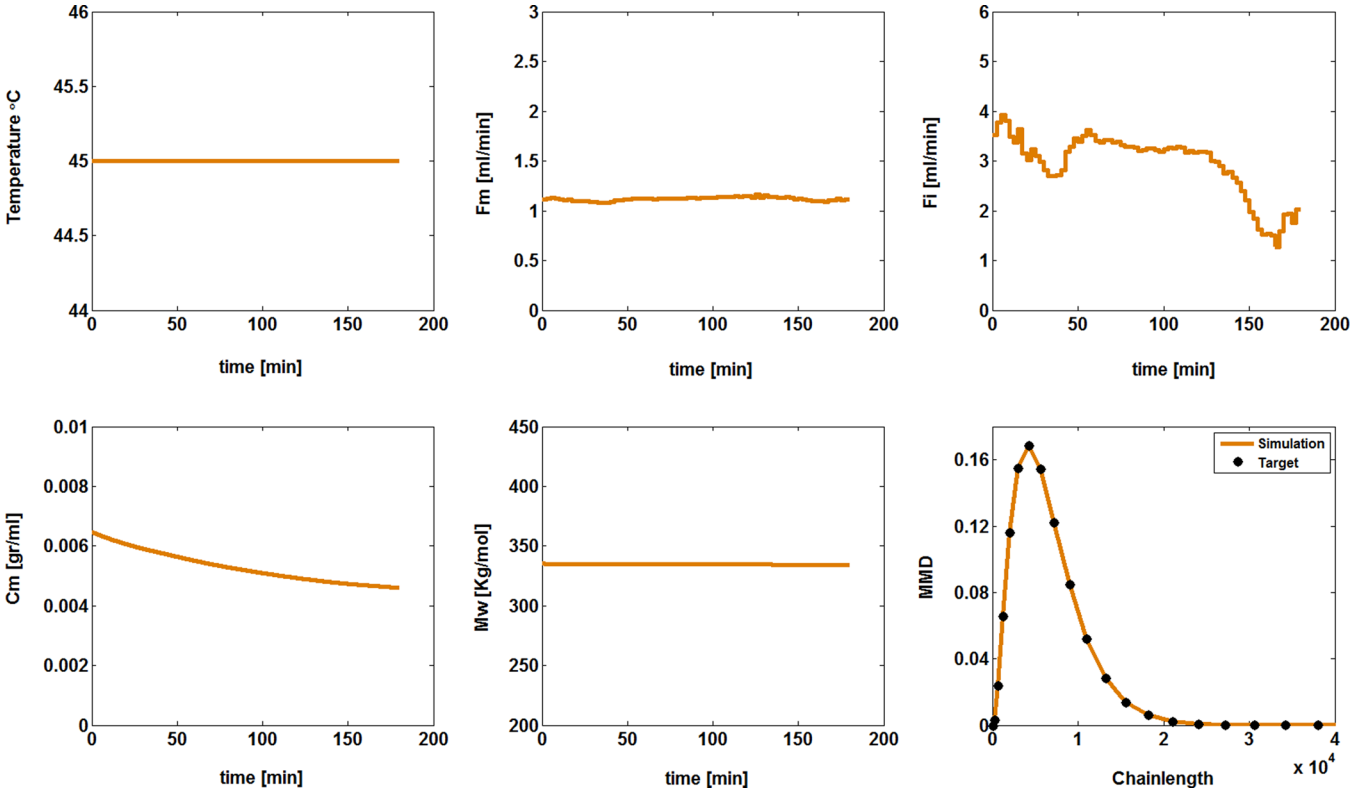

Figure 2. Simulation results using the optimal trajectories for the constant M_w scenario.

were constant over a couple of consecutive intervals. So, although the profiles look continuous, the solution is still a piece-wise constant trajectory. For the sake of clarity, the enlarged plots of monomer and initiator flows are shown in Figure 3. As the figures are showing, the trajectories in these cases also follow a piecewise constant function.

Case 3: Increasing M_w. In the previous case studies, it was observed how to keep M_w constant by keeping a constant ratio

DOI: 10.1021/acs.iecr.7b01074
Ind. Eng. Chem. Res. 2017, 56, 7322−7335

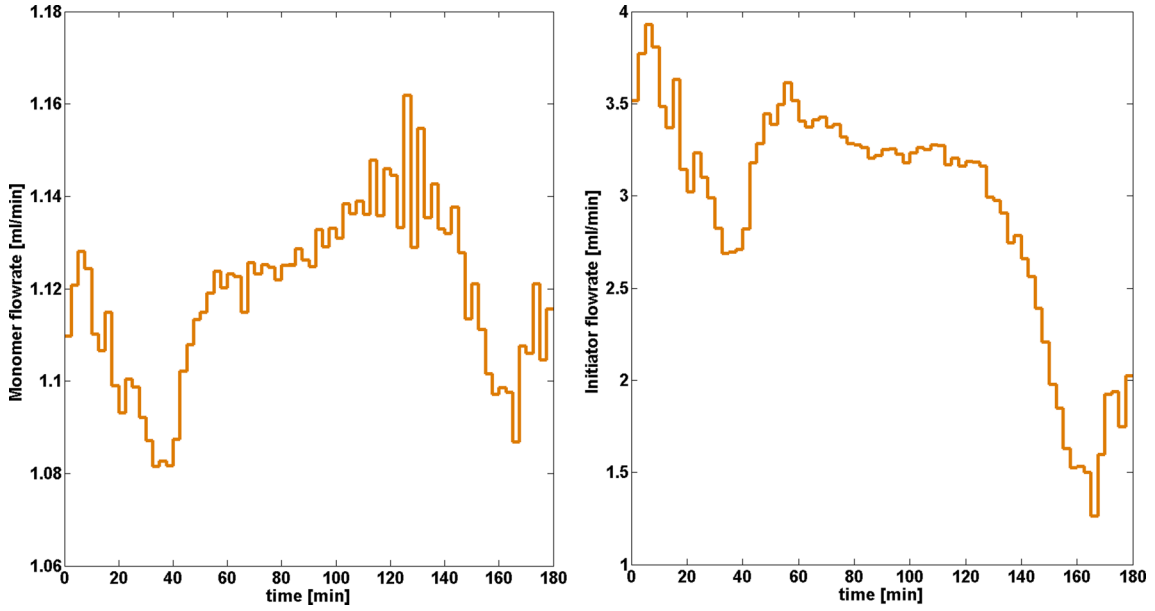

Figure 3. Monomer and initiator profiles after enlargement of plots.

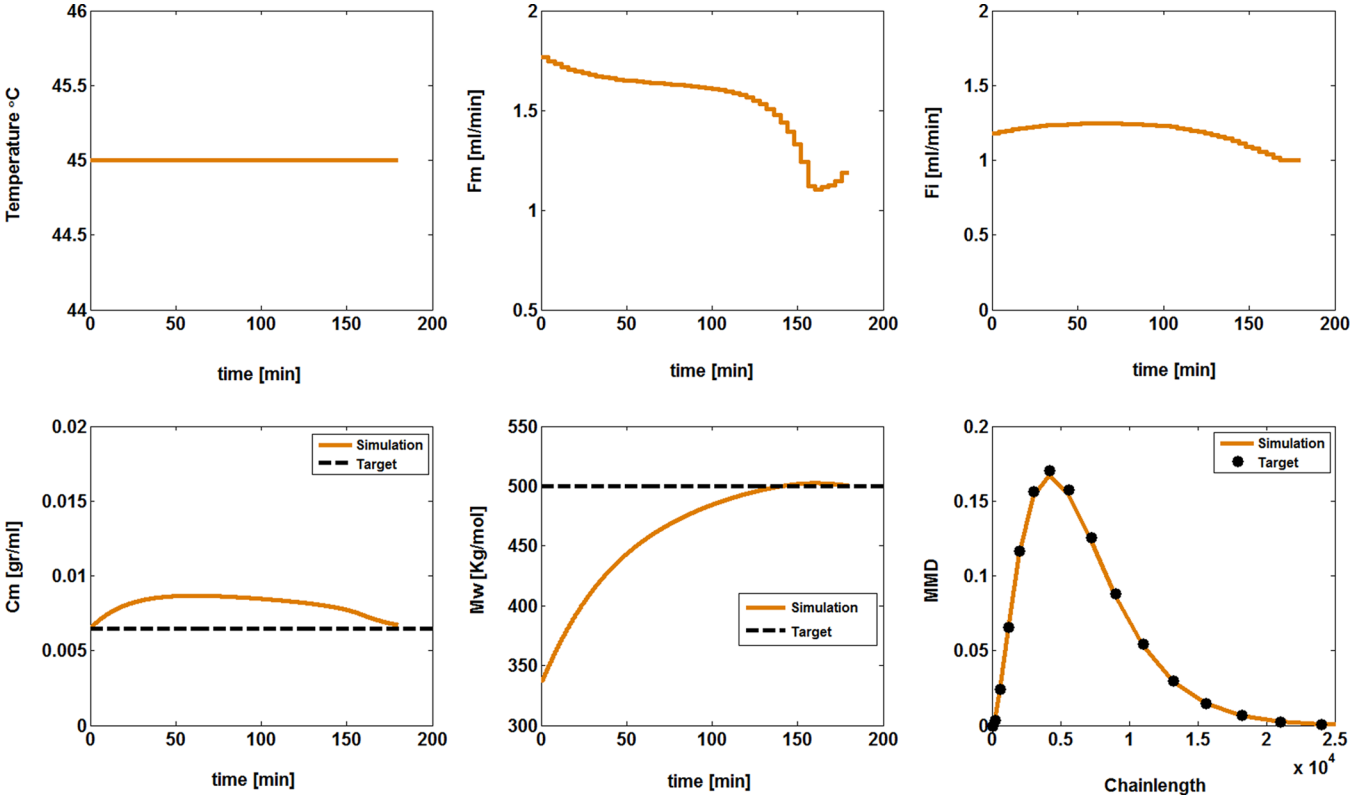

Figure 4. Simulation results applying the optimal trajectories for the increasing M_w scenario.

between the monomer and free radical concentrations. It was also shown how to have a decreasing trend of M_w starting from a high value of M_w and reducing the monomer feed while increasing the initiator flow. To complete our analysis, here we focus on an optimization scheme which could lead to an increasing trend for M_w. As a rule of thumb, this requires a higher monomer flow compared with the initiator, which was injected into the reactor in case 1, which causes the reactor volume exceeding the maximum value allowed. To meet the optimization constraints, like in the previous case, the flows were diluted and the monomer concentration was maintained higher with respect to initiator at the corresponding flow. As a result, the monomer feed rate will have a more significant effect on the M_w and is able to increase the weight average. The objective function in this case is formulated as follows:

$$J = w_1\left(\frac{X_f}{X_t} - 1\right)^2 + w_2\left(\frac{M_{w,f}}{M_{w,t}} - 1\right)^2 + w_3 \sum_{nc}^{i=1}\left(\frac{f_{i,f}}{f_{i,t}} - 1\right)^2 \quad (19)$$

DOI: 10.1021/acs.iecr.7b01074
Ind. Eng. Chem. Res. 2017, 56, 7322−7335

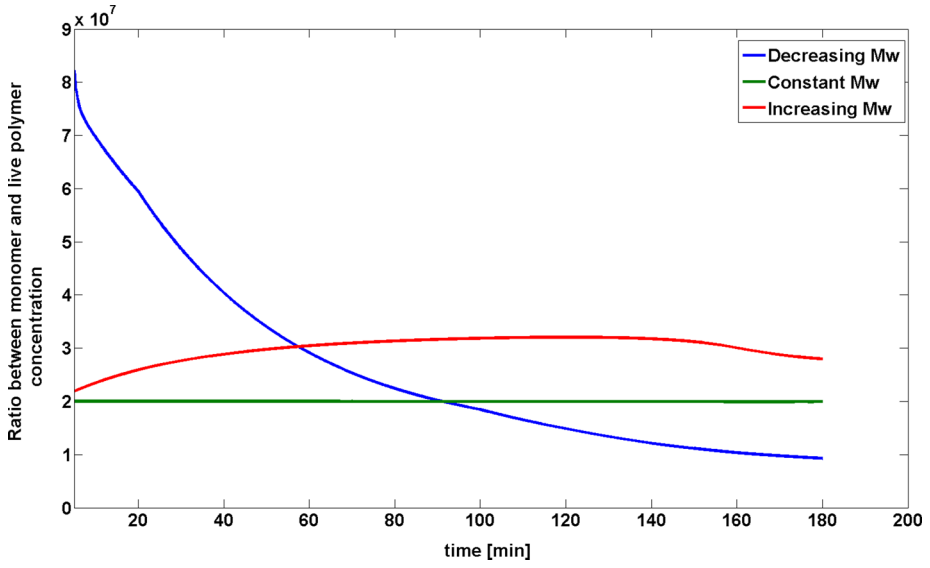

Figure 5. Computation of the ratio between monomer and live polymer concentration, C_m/P_0, for different M_w trajectories.

The term N_{mf}, total amount of monomer injected to the reactor, was eliminated from the objective function to give the extra degree of freedom for adding monomer. Results are shown in Figure 4. M_w increases successfully during the simulation and reaches the desired target. There is also a good match in the monomer concentration and MMD results between the targets and simulation profiles. It should be mentioned that, although in this case initiator and monomer flow do not change considerably during the process, by changing the feed concentration as explained earlier, an increase in C_m and as a result in the instantaneous number-average molar mass happens. This is also demonstrated in Figure 4 in the monomer concentration profile. More moles of monomer are feeding in than are being polymerized, so the monomer concentration goes up, and thus the M_w.

To summarize this section, Figure 5 compares the computed ratio between the monomer and live polymer concentration for the three optimization case studies discussed. It is clear that controlling the ratio between monomer and live polymer concentration can affect the final M_w results.

Feedback Control of M_w. To control the optimal M_w trajectory, a conventional proportional-integral (PI) controller is designed where M_w is controlled by manipulating monomer flow rate. The choice of the manipulated variable for the feedback control of M_w is based on the input effects on the controlled variable in terms of gain and response time. From different simulation analyses, the monomer flow has been shown to better fit the requirements than initiator flow. The feedback control uses a PI-like algorithm, which is expressed mathematically as follows:

$$u_n = \bar{u} + k_c\left[e_n + \frac{\Delta t}{\tau_i}\sum_{n}^{k=1} e_k\right] \tag{20}$$

where u_n denotes the value for input variables (monomer flow) at each time instant which is sent to the pump. k_c and τ_i are the proportional gain and integral time constants of the controller. These parameters are tuned using different simulations with the model, and optimum values for them are selected, which vary for each experiment.

An alternative approach is to use the velocity form of eq 20 in which the change in controller output is calculated and applied instead of the output value. When eq 20 is written for the $n-1$ sampling time and subtracted from eq 20, straightforward calculation will lead to the following form:

$$\Delta u_n = k_c\left[(e_n - e_{n-1}) + \frac{\Delta t}{\tau_i}e_n\right] \tag{21}$$

The velocity form has two main advantages over the position form. First, it intrinsically contains some provisions for antireset windup since the summation of errors is not explicitly calculated. The antireset windup could be considerably high for M_w because the time constant of the process is quite large and the response is slow. Second, for velocity control algorithms, applying the controller in automatic mode, that is, switching it from manual operation, does not require any initialization of the output $\bar{u}$. This is also a prerequisite in this work since all the control experiments start based on the optimization trajectory for the first 15−20 min of the experiment, and then once the data from ACOMP stabilizes, the controller starts to provide corrective actions.

Nonlinear (Linearizing) Control of Monomer Concentration. From previous discussions, it is clear that the main objective in controlling polymerization reactors is to control M_w and indirectly the MMD. Since online measurement of monomer concentration is also available by ACOMP, an effort was made to control the total amount of monomer and as a result the monomer concentration inside the reactor by manipulating the monomer flow (F_m). The control strategy is based on the input−output linearizing geometric approach, which takes into account the nonlinear dynamic of the process, formalized in the general dynamic model. Unfortunately, due to the complex relationship between M_w and F_m, no such formulation can be designed for controlling M_w.

The principle of the linearizing method is to structure a control law in which the tracking error follows a specified stable linear differential equation known as the reference model.[26,27] The control algorithm can be explained in three steps. First the input−output model should be derived by appropriate manipulation of the general dynamic model. This provides

DOI: 10.1021/acs.iecr.7b01074
Ind. Eng. Chem. Res. 2017, 56, 7322−7335

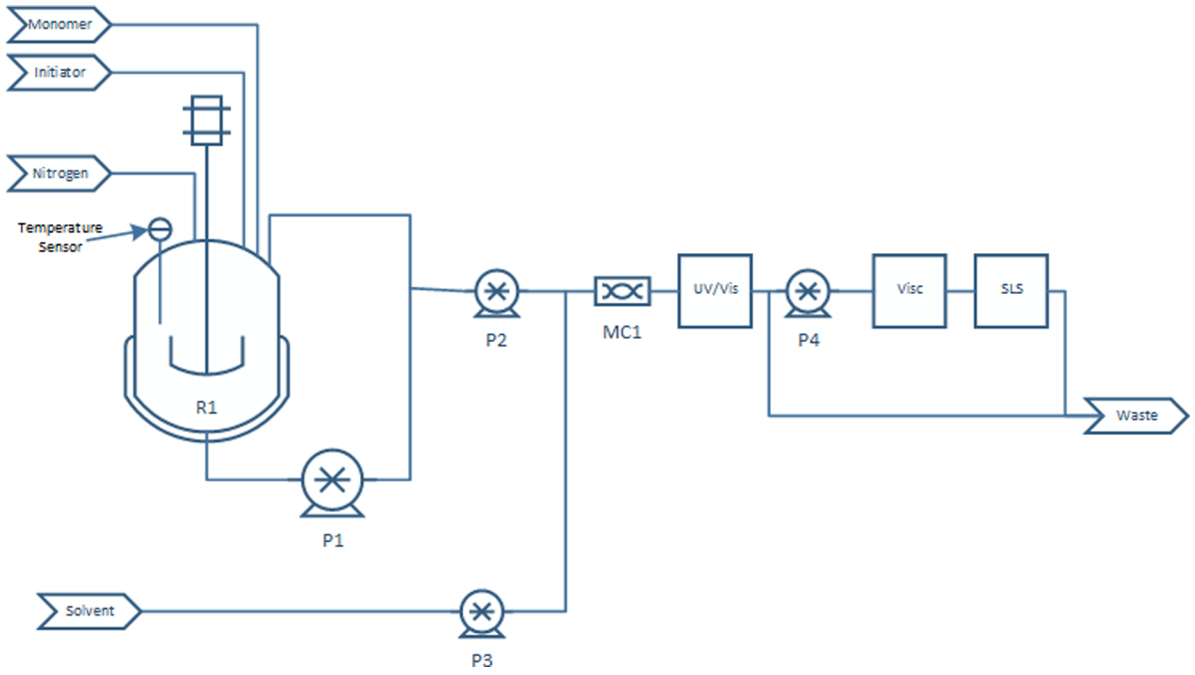

Figure 6. Schematic of ACOMP process flow diagram, showing the steps for extraction, dilution, and typical multidetectors.

an explicit relation between the manipulated variables and the control objectives which takes the form of an nth order differential equation:

$$\frac{d^n y}{dt^n} = f_0(t) + u(t) f_1(t) \tag{22}$$

with n being the relative degree of the input/output model. Depending on the control and manipulated variables, $f_0(t)$ and $f_1(t)$ could be highly complex functions of the model parameters. However, the relation is always linear with respect to the manipulated variable. Second, a stable linear reference model of the tracking error is selected. The model determines how we desire the tracking error to decrease and is presented as follows:

$$\sum_{n}^{j=0} \lambda_{n-j} \frac{d^j}{dt^j}[y^*(t) - y(t)] = 0 \quad \lambda_0 = 1 \tag{23}$$

The coefficients λ_{n-j} are tuning coefficients which should be selected so that the differential eq 23 is stable. Finally, the control design consists of calculating the control action $u(t)$ such that the input−output model exactly matches the reference model. Using eq 22 and substituting for $^{d^n y}/_{dt^n}$ in eq 23, the solution for $u(t)$ can be obtained.

$$u(t) = \frac{1}{f_1(t)}\left[-f_0(t) + \sum_{j=0}^{n} \lambda_{n-j} \frac{d^j}{dt^j}[y^*(t) - y(t)] + \frac{d^n y^*}{dt^n}\right] \tag{24}$$

The formalism of the nonlinear controller using F_m as a manipulated variable is considered in this case. The relative degree of F_m and N_m is 1 according to eq 1. Using eq 24 and substituting for $^{dN_m}/_{dt}$ from eq 1, an explicit relation for monomer feed rate $F_m(t)$ can be obtained with respect to known variables:

$$F_m = \left(\frac{dN_m^*}{dt} - \lambda_p[N_m^* - N_{mp}] - \lambda_i[\int (N_m^* - N_{mp})\, dt] + F_{out} C_m + (k_p) C_p N_m\right) \Big/ C_{mf} \tag{25}$$

where N_m^* is the desired/target optimal known trajectory for the total amount of monomer obtained from dynamic optimization. It is worth noting that a similar approach is also possible by using the initiator flow as a manipulated variable; however, in this case, the relative degree is 2, thus leading to a more complex (although explicit) relationship.

3. EXPERIMENTAL IMPLEMENTATION OF THE FEEDBACK CONTROL SCHEME USING ACOMP

Materials and Methods. The starting solutions for the reactor and feed pump reservoirs were made from powder acrylamide monomer, ≥99%, and powder potassium persulfate (KPS) initiator, ≥99%, purchased from Sigma-Aldrich, and dissolved in DI water. The starting solutions for the reactor and feed pump reservoirs were stirred and purged with ultrahigh purity nitrogen at 100 cm^3/min starting 45 min prior to initiating the reaction. The reactor is then heated to the desired optimal temperature, unless specified otherwise, and then the reaction is initiated by the addition of KPS powder.

Experimental Apparatus—ACOMP System. Solution polymerization reactions were performed in a 1.5 L reactor while being continuously monitored using ACOMP. The primary components of the experimental setup are shown in Figure 6. A continuous stream of reactor contents is removed at the rate of 0.5 mL/min, diluted 80 times with DI water, homogenized in a mixing chamber, and then measured by ultraviolet−visible (UV−vis) absorption spectroscopy, viscometry, and multiangle laser light scattering (MALS) detectors. UV−vis absorption

DOI: 10.1021/acs.iecr.7b01074
Ind. Eng. Chem. Res. 2017, 56, 7322−7335

spectroscopy at 245 nm was used to determine the monomer and polymer concentrations. When the polymer concentration is known, M_w can then be calculated from the SLS data. Further details on ACOMP's functionality and methodology is available in the literature.[23,28]

Controller Implementation. To test the performance of the controller, a controller module was formulated and implemented in Python, which interacts continuously via Excel using the optimal trajectories provided by gPROMS. The controller can communicate with the plant (ACOMP) at the same time, performing the control action at a regular number of sampling times. A flow diagram of the controller implementation is shown in Figure 7. The controller was initiated by reading

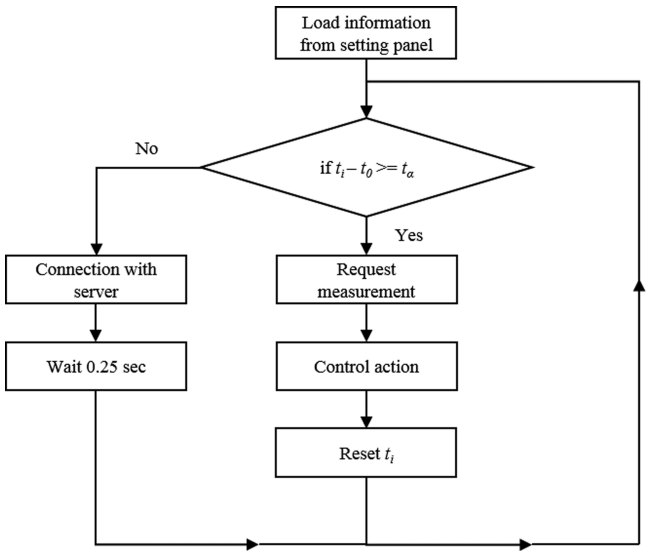

Figure 7. Flow diagram of the control implementation.

information from the setting panel including set-point recipe, control parameters, and ACOMP server information. A main loop was designed to govern the communication with the ACOMP server at a frequency of 4 Hz. Once the time interval was over the threshold (2.5 min per action), the most recent measurement of the set-point variable was requested from ACOMP server before the discrete control action was activated.

The set point trajectory is the optimal trajectory obtained during the optimization studies. While one of the input manipulated variables is adjusted by the feedback controller, all other inputs are applied according to the optimal recipe obtained during the optimization. Monomer is the manipulated variable, and M_w is chosen as the parameter to control while its controllability is analyzed with respect to monomer flow. Monomer concentration and MMD profiles are also illustrated and compared with their optimal trajectories. Figure 8 shows a schematic representation of the approach followed in the simulation and experimental studies. The proposed framework for implementing control in a different environment than the model serves two purposes. First, it shows that the function of the controller can be calculated either from the process and/or from the nominal (optimal) conditions. Second, once the controller is implemented in a different environment, it allows a straightforward move from the simulation studies to control the actual process. The Python environment for implementation was selected since it is easily adaptable and compatible to the modeling environment as well as any control system. However, it is envisaged that a final version of the control module will be developed in the Python environment, using a single module for all possible control strategies with a switching option for selecting the inputs and outputs of the controller.

4. RESULTS AND DISCUSSION

This section will show the results obtained for all the optimization and control techniques studied in the previous parts. To demonstrate the feasibility of the proposed strategies, different objective functions, which were formulated in the optimization section, are validated experimentally using data from ACOMP. Building on these results, three control experiments are designed in which the controller set-points are the optimal trajectories obtained from the simulation. The feedback control is achieved in all cases using the monomer flow as the manipulated variable to control M_w. All other input profiles, namely the temperature and initiator flow rates, are set equal to their corresponding optimal trajectories, obtained during optimization. For all closed-loop cases, the system is initially started using the optimal input trajectories, and after 20 min, the controllers are switched on to provide corrective actions. This is to allow enough polymerization to occur for the SLS detector signal to be larger than the baseline noise. Table 4 gives a summary of all the various optimization and control experiments, including the initial loading, feed rate concentrations, and control parameters for each reaction.

Case 1: Decreasing M_w. Figure 9 shows the experimental results for the open-loop (optimization) experiment in term of M_w which is displayed in gray solid line. Optimization targets are also displayed using dashed lines for comparison between the model prediction and experimental data. The experimental profile obtained from ACOMP is pretty close to the computed target M_w, with a slight difference due to the model inaccuracy and disturbances in the system. The trend of M_w at the beginning of the optimization experiment is different from what was expected from the model, which is due to the time the initiator was added to the reactor. In the simulation, it is considered that the reactor is heated up to the desired temperature after the initiator is added to the system, while during the real experiment the reactor was heated up first and the initiator was added to initiate the reaction. This causes a lower M_w at the beginning of the reaction.

As observed in the M_w results, there has been a mismatch between the computed M_w which was predicted from the model and the experimental data obtained from ACOMP during the optimization experiment. Given that, it is desired to apply the controller, which was explained in detail in section 2. After preliminary testing of the controller's performance using the simulations of the nonlinear model, the proposed control design was implemented on the ACOMP system. Optimal trajectories of M_w from the simulation were used as the set-point of the controller. Since there was a rather high difference between the experimental results and the simulation in the previous case and in order to compensate for that, the controller is required to inject higher amounts of monomer into the system to increase the M_w. Using the knowledge from the optimization studies, the experiment was performed at a slightly lower temperature to avoid injection of a high amount of monomer. This will result in a higher M_w and reduces the amount of monomer which is necessary to be inserted into the system. From the monomer flow profile in Figure 9, it is noticed that the controller stops the monomer feed pump at $t \cong 20$ min, and the controller is able to keep M_w close to the desired set point. There is an excellent

DOI: 10.1021/acs.iecr.7b01074
Ind. Eng. Chem. Res. 2017, 56, 7322−7335

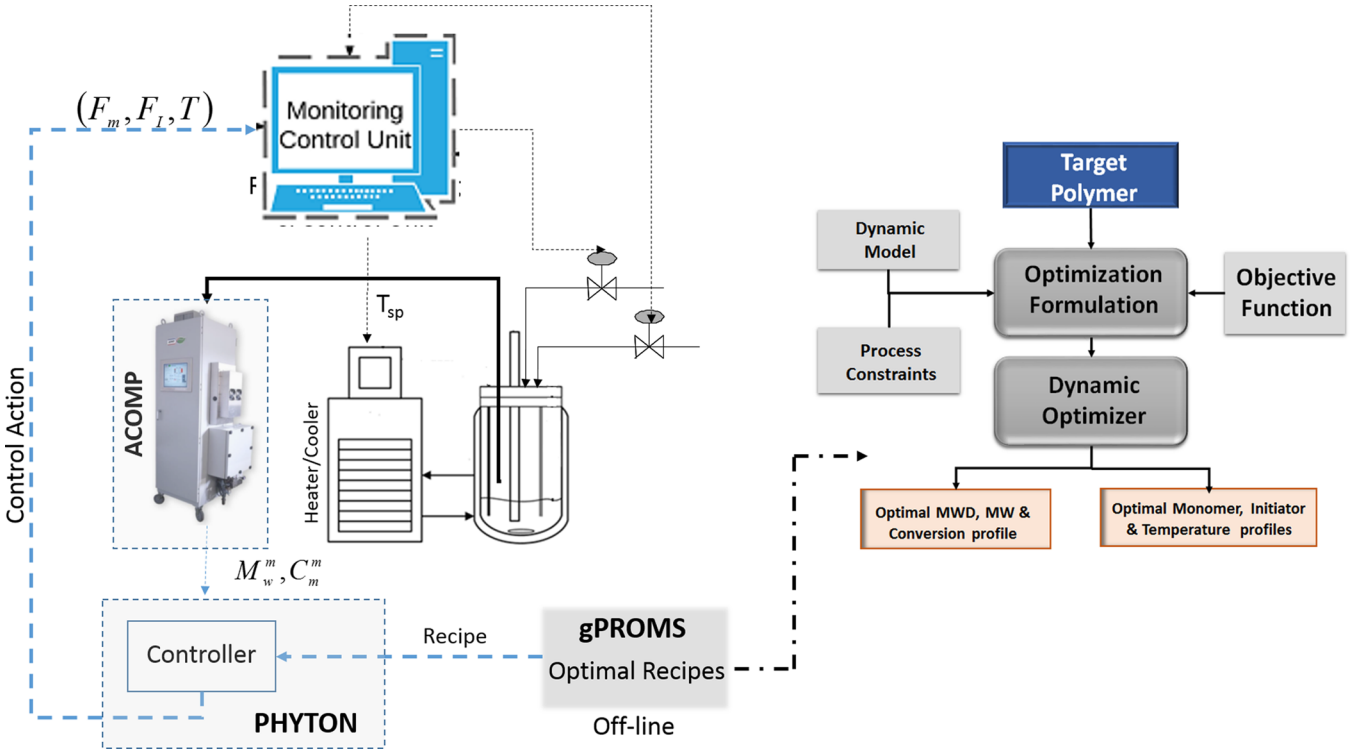

Figure 8. Schematic representation of the proposed approach for optimization and control of the system.

Table 4. Summary of All the Optimization and Control Experiments

exp. #	exp. description	N_m [mol]	N_s [mol]	N_i [mol]	C_{if} [mol/m^3]	C_{mf} [mol/m^3]	k_p [prop. gain]	τ_I [int. gain]
1	optimization decreasing, M_w	0.3	50	0.005	110.9796	7175.014	N/A	N/A
2	feedback control decreasing, M_w	0.3	50	0.005	110.9796	7175.014	5×10^{-9}	1×10^{11}
3	optimization const., M_w	0.05	30	0.008	3.699	1406.866	N/A	N/A
4	feedback control const., M_w	0.05	30	0.008	3.699	1406.866	2×10^{-8}	1.5×10^{10}
5	optimization increasing, M_w	0.05	30	0.008	3.699	1406.866	N/A	N/A
6	feedback control increasing, M_w	0.05	30	0.008	3.699	1406.866	2×10^{-8}	1.5×10^{10}
7	feedback control, C_m	0.3	50	0.005	110.9796	7175.014	N/A	N/A

match between the experimental data and the desired set-point after around 60 min and beyond.

Also, to determine the final MMD, gel permeation chromatography (GPC) was performed on the end products of the control experiment. Results are presented as the mass fraction of polymers with different chain length intervals. The final distribution of polymers is quite close to what the model predicts. The experimental results also show a higher mass fraction of polymers with longer chain lengths, which is in agreement with the M_w data.

Case 2: Constant M_w. Next, experimental validations are performed for the case of targeting a constant M_w. Figure 10 displays the comparison between the experimental values of M_w and the values computed by the model. There is a slight difference between the desired target and experimental results in the open-loop experiment. On the other hand, the controller is again successful in holding M_w close to its desired target. Like in the previous case, the optimal input trajectory of monomer flow rate is modified by the controller to bring the process to the target M_w. There is also a very good match between the final MMD results and the model. It is worth noticing that keeping M_w constant along the reaction will result in smaller distribution width compared with the previous case.

Case 3: Increasing M_w. The obtained optimization recipe is also validated for the increasing trajectory of M_w. Results for the M_w and MMD are reported in Figure 11. The M_w results from the optimization experiment are in good agreement with the model prediction, following exactly the trend with a small deviation due to model uncertainties. In Figure 11, a comparison between the monomer flow profiles shows that the controller almost follows the same trajectory as the optimal trend predicted in the simulation in order to follow the optimal path of M_w This result is expected since there was already a good agreement in the open loop results for M_w. There is also a very good match in the final MMD results.

Model-Based Linearizing Control of Total Amount of Monomer. Additional experiments were performed to test the functionalities of the nonlinear controller. Similar to previous cases, all other input trajectories were set equal to their corresponding optimal trajectories obtained during the optimization. The target total amount of monomer (N_m^*) as required by eq 25 was also obtained from the optimization results. The operating scenario selected for this test had a decreasing M_w trend. Figure 12 shows the closed loop results in terms of the control variable (C_m), manipulated variable (F_m), and (M_w) trajectories. The monomer flow trajectory follows the same trend as the optimal trajectory, while small changes are applied due to model uncertainties. The total amount of monomer added to the reactor is rather small, and there is almost a 100% conversion to polymer

DOI: 10.1021/acs.iecr.7b01074
Ind. Eng. Chem. Res. 2017, 56, 7322−7335

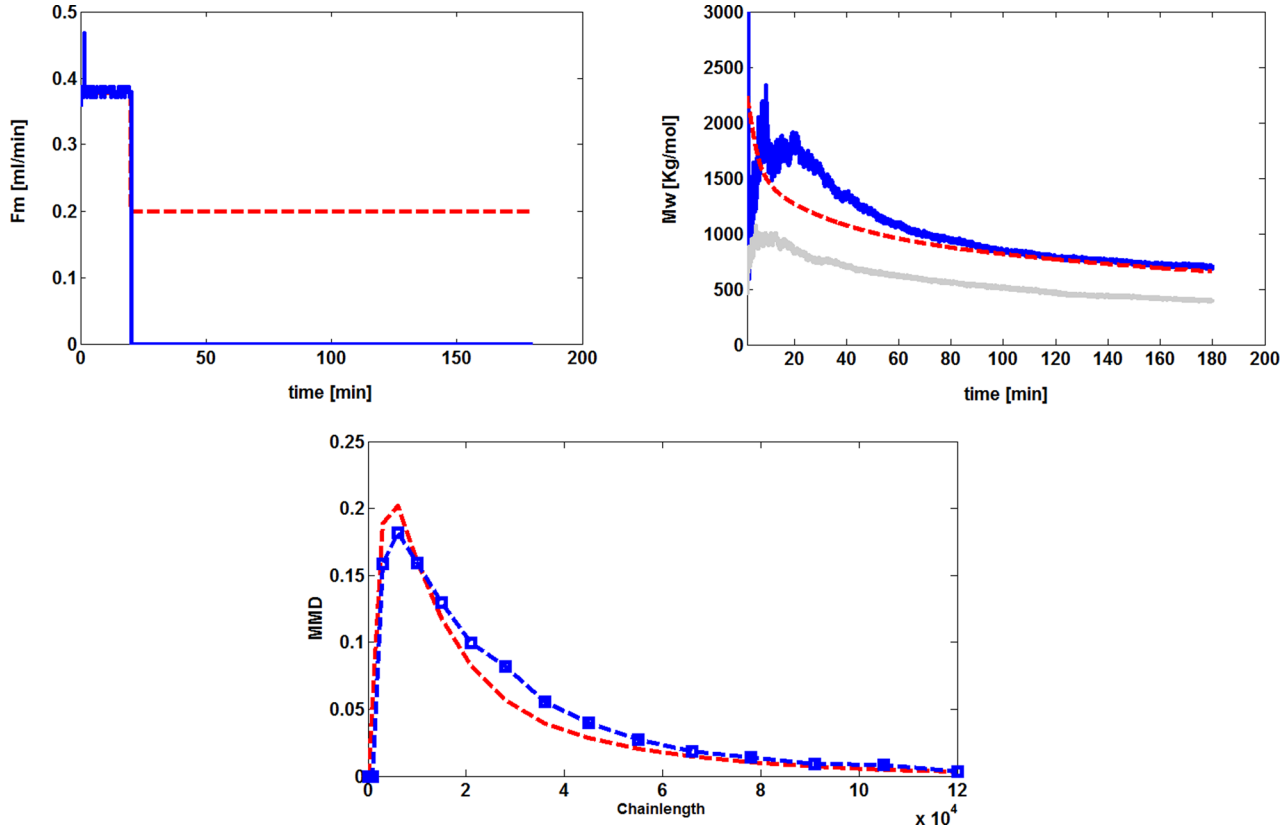

Figure 9. Experimental results for the open-loop and closed-loop cases for decreasing M_w scenario. Upper panel: monomer flow (left), weight-average molar mass (right). Lower panel: molar mass distribution. Red: target (simulation). Gray: open loop. Blue: closed loop.

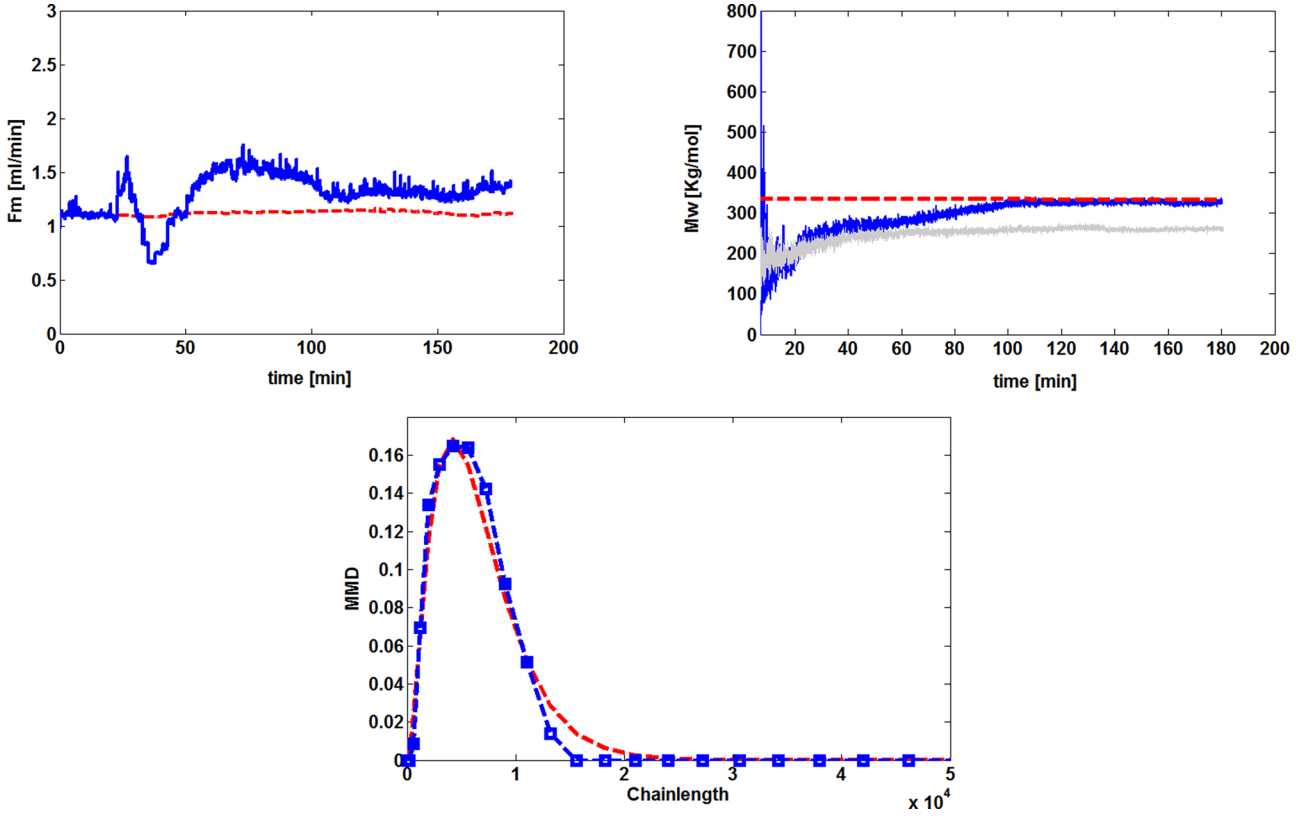

Figure 10. Experimental results for the open-loop and closed-loop cases for constant M_w scenario. Upper panel: monomer flow (left), weight-average molar mass (right). Lower panel: molar mass distribution. Red: target (simulation). Gray: open loop. Blue: closed loop.

DOI: 10.1021/acs.iecr.7b01074
Ind. Eng. Chem. Res. 2017, 56, 7322−7335

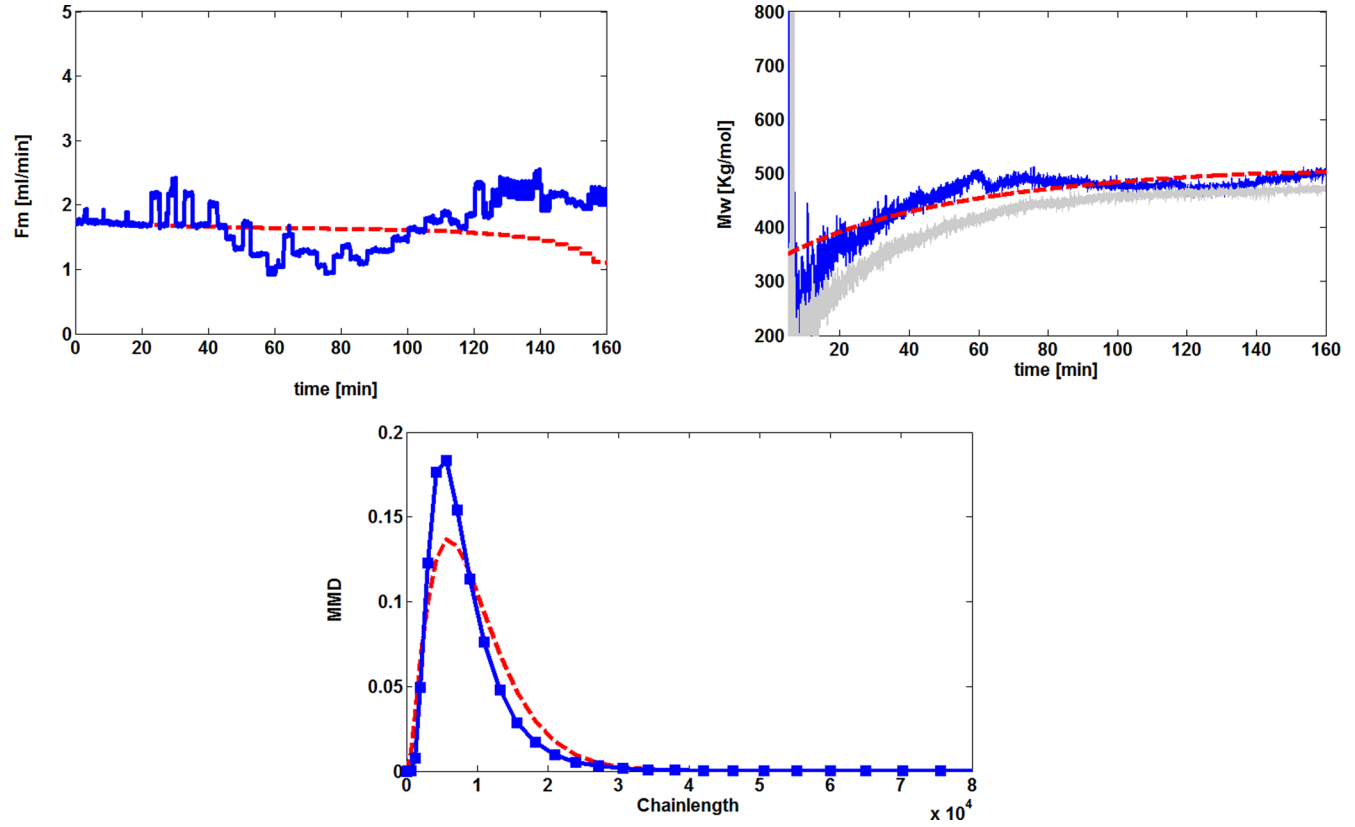

Figure 11. Experimental results for the open-loop and closed-loop cases for increasing M_w scenario. Upper panel: monomer flow (left), weight-average molar mass (right). Lower panel: molar mass distribution. Red: target (simulation). Gray: open loop. Blue: closed loop.

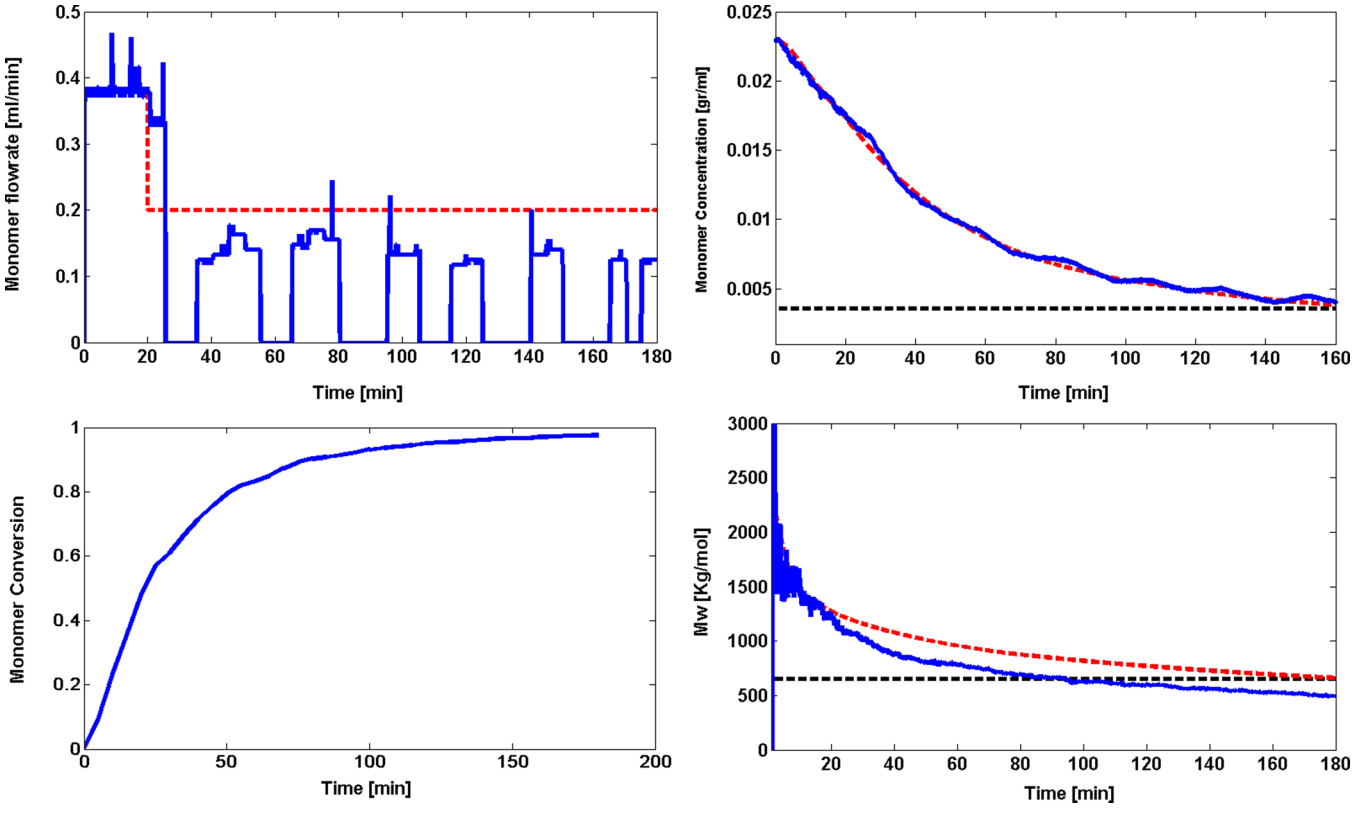

Figure 12. Experimental results for the closed-loop experiment controlling C_m. Upper panel: monomer flow (left), monomer concentration (right). Lower panel: conversion (left), weight-average molar mass (right). Red: target (simulation). Blue: closed loop.

DOI: 10.1021/acs.iecr.7b01074
Ind. Eng. Chem. Res. 2017, 56, 7322−7335

Table 5. Target Values of the Chain Length Fractions for the Different Optimization Studies

chain length fraction/ optimization #	1	2	3
f_1	0.003208614	0.003468878	0.003393961
f_2	0.02077042	0.024174135	0.023685269
f_3	5.02×10^{-02}	0.06591914	0.06473725
f_4	0.09715878	0.11617943	1.14×10^{-01}
f_5	0.101271095	0.15511458	0.15347804
f_6	0.10296918	0.1684133	0.16749695
f_7	0.087787844	0.15443532	0.15453357
f_8	0.08011126	0.12234499	0.12328713
f_9	0.07173572	0.08496359	0.08630395
f_{10}	0.05814185	0.05224137	5.35×10^{-02}
f_{11}	0.051371576	0.028642986	2.96×10^{-02}
f_{12}	0.042185819	0.014077419	0.014729873
f_{13}	0.034030668	0.006226718	0.006592644
f_{14}	0.026958221	0.002486401	0.002666338
f_{15}	0.020975091	0.000898513	9.77×10^{-04}
f_{16}	0.016039185	0.000294427	3.25×10^{-04}
f_{17}	0.012066454	8.76257×10^{-05}	9.82×10^{-05}
f_{18}	0.008943499	2.37174×10^{-05}	2.70×10^{-05}
f_{19}	0.006542024	5.84482×10^{-06}	6.78×10^{-06}
f_{20}	0.00473201	1.31266×10^{-06}	1.55×10^{-06}
f_{21}	0.003391765	2.68882×10^{-07}	3.25×10^{-07}
f_{23}	0.002414262	5.02673×10^{-08}	6.33×10^{-08}
f_{24}	0.00171003	8.58075×10^{-09}	1.22×10^{-08}
f_{25}	0.001207391	1.33685×10^{-09}	3.14×10^{-09}
f_{26}	0.000850943	1.88814×10^{-10}	1.67×10^{-09}
f_{27}	0.000599126	2.27606×10^{-11}	1.45×10^{-09}
f_{28}	0.000421519	8.27203×10^{-13}	1.42×10^{-09}
f_{29}	0.000296267	-1.81985×10^{-12}	1.42×10^{-09}
f_{30}	0.000207885	-2.11187×10^{-12}	1.42×10^{-09}
f_{31}	0.000145483	-2.14133×10^{-12}	1.42×10^{-09}
f_{32}	0.000101428	-2.14405×10^{-12}	1.42×10^{-09}
f_{33}	7.03657×10^{-05}	-2.14428×10^{-12}	1.42×10^{-09}
f_{34}	4.85224×10^{-05}	-2.1443×10^{-12}	1.42×10^{-09}
f_{35}	3.32258×10^{-05}	-2.1443×10^{-12}	1.42×10^{-09}

as the conversion profile displays. Clearly, the performance of the controller is excellent, forcing the monomer concentration to follow closely the optimal profile. However, as can be seen in the M_w diagram, there is quite a big difference (around 15%) between the simulation and experimental results, meaning that even perfect control on monomer concentration does not guarantee achieving the optimal M_w target.

5. CONCLUSION

Control of polymerization processes has been challenging due to the complexity of the polymeric systems and lack of online measurement of polymer properties. In this paper, a hierarchical approach for controlling polymerization reactors for the case of weight-average molar mass was presented. The work structure consisted of (1) developing a first principle model for the weight-average molar mass and molar mass distribution, which was validated using the experimental data, (2) formulating a dynamic optimization problem for different case studies to obtain optimal profiles of the process decision variables, (3) constructing a nonlinear model and a modified simple version of the PI controller, and (4) validating the optimal profiles experimentally.

Overall, the output-feedback system performs well and shows good robustness properties under a range of operating conditions, allowing full control of M_w and MMD. Current work is underway to incorporate dynamic filtering into the proposed architecture. This will not only provide improved (filtered) measurement but also extend the functionalities of ACOMP through (measured corrected) predictions of unmeasured variables such as number-average molar mass, polydispersity, and real-time variations of the MMD.

APPENDIX A

AUTHOR INFORMATION

Corresponding Author

*Tel.: +1225-578-1377. E-mail: Jose@lsu.edu.

ORCID

Jose A. Romagnoli: 0000-0003-3682-1305

Notes

The authors declare no competing financial interest.

ACKNOWLEDGMENTS

The information, data, or work presented herein was funded in part by the Office of Energy Efficiency and Renewable Energy (EERE), U.S. Department of Energy, under Award Number DE-EE0005776. Additional support came from NSF EPS-1430280 and Louisiana Board of Regents. The authors acknowledge support from Mr. Phong Pham for automation and integration and Mr. Colin Bellmore for software development.

NOTATION

A_d = pre exponential factor for propagation kinetic rate constant [m^3/mol·min]
A_p = pre exponential factor in propagation kinetic rate constant [m^3/mol·min]
A_t = pre exponential factor in chain transfer to monomer rate constant [m^3/mol·min]
C_i = concentration of initiator inside the reactor, mol/m^3
C_{if} = initiator concentration in the monomer flow rate, [mol/m^3]
C_m = concentration of monomer inside the reactor, mol/m^3
C_{mf} = monomer concentration in the monomer flow rate, [mol/m^3]
C_s = concentration of solvent inside the reactor, mol/m^3
C_{sif} = solvent concentration in the monomer flow rate, [mol/m^3]
C_{smf} = solvent concentration in the monomer flow rate, [mol/m^3]
E_p = activation energy in propagation kinetic rate constant, J/mol
E_{fm} = activation energy in in chain transfer to monomer rate constant
f = initiator efficiency
F_i = flow rate of initiator to the reactor, [m^3/min]
F_{out} = extraction flow rate out of the reactor for sampling purposes, [m^3/min]
F_m = flow rate of monomer to the reactor, [m^3/min]
k_d = decomposition rate constant of the initiator, [1/min]
k_{fm} = rate constant for chain transfer to monomer reactions, [m^3/mol·min]
k_{fs} = rate constant for chain transfer to solvent reactions, [m^3/mol·min]
k_p = propagation rate constant, [m^3/mol·min]
k_{tc} = rate constant for termination by combination reactions, [m^3/mol·min]

DOI: 10.1021/acs.iecr.7b01074
Ind. Eng. Chem. Res. 2017, 56, 7322−7335

k_{td} = rate constant for termination by disproportionation reactions, [m^3/mol·min]
M_n = number-average molar mass, kg/mol
M_w = weight-average molar mass, kg/mol
N_i = total amount of initiator inside the reactor, mol
N_m = total amount of monomer inside the reactor, mol
N_{m0} = initial amount of monomer inside the reactor, mol
N_{mf} = total amount of monomer added to the reactor from the flow rates, mol
N_s = total amount of solvent inside the reactor, mol
P_0 = concentration of live polymer in the reactor, mol/m^3
T = temperature of the reactor, K
t = time, min
V = volume of the material inside the reactor, [m^3]
w_m = molecular weight of monomer, kg/mol
w_i = molecular weight of initiator, kg/mol
w_s = molecular weight of solvent, kg/mol
X = monomer conversion

Greek Letters

λ_0 = 0th moment of the MWD, mol/m^3
λ_1 = first moment of the MWD, mol/m^3
λ_2 = second moment of the MWD, mol/m^3
α = probability of propagation
ρ_m = density of monomer, kg/m^3
ρ_i = density of initiator, kg/m^3
ρ_s = density of solvent, kg/m^3

REFERENCES

(1) Srinivasan, N.; Kasthurikrishnan, N.; Cooks, R. G.; Krishnan, M. S.; Tsao, G. T. Online monitoring with feedback-control of bioreactors using a high ethanol tolerance yeast by membrane introduction mass-spectrometry. *Anal. Chim. Acta* **1995**, *316*, 269−276.
(2) Eaton, J. W.; Rawlings, J. B. Feedback-control of chemical processes using online optimization techniques. *Comput. Chem. Eng.* **1990**, *14*, 469−479.
(3) Ray, W. H. Polymerization reactor control. *Ieee Transactions on Control Systems Technology* **1986**, *6*, 3.
(4) Nguyen, T.Q.; Kausch, H. H. Molecular weight distribution and mechanical properties. *Mechanical Properties and Testing of Polymers*; Polymer Science and Technology Series, Springer: Berlin, 1999, Vol 3, pp 143−150.
(5) Isayev, A. I.; Palsule, S. *Encyclopedia of polymer blends, volume 2: Processing*; Wiley: Hoboken, NJ, 2011.
(6) Voyiadjis, G. Z.; Samadi-Dooki, A. Constitutive modeling of large inelastic deformation of amorphous polymers: Free volume and shear transformation zone dynamics. *J. Appl. Phys.* **2016**, *119*, 119.
(7) Cho, H. S.; Chung, J. S.; Lee, W. Y. Control of molecular weight distribution for polyethylene catalyzed over ziegler-natta/metallocene hybrid and mixed catalysts. *J. Mol. Catal. A: Chem.* **2000**, *159*, 203−213.
(8) Heidemeyer, P.; Pfeiffer, J. Special requirements on compounding technology for bimodal polyolefines and their industrial application. *Macromol. Symp.* **2002**, *181*, 167−176.
(9) McKeen, L. *The Effect of Temperature and Other Factors on Plastics and Elastomers*. William Andrew Inc: Norwich, NY, 2008.
(10) Yoon, W. J.; Kim, Y. S.; Kim, I. S.; Choi, K. Y. Recent advances in polymer reaction engineering: Modeling and control of polymer properties. *Korean J. Chem. Eng.* **2004**, *21*, 147−167.
(11) Kreft, T.; Reed, W. F. Predictive control and verification of conversion kinetics and polymer molecular weight in semi-batch free radical homopolymer reactions. *Eur. Polym. J.* **2009**, *45*, 2288−2303.
(12) Crowley, T. J.; Choi, K. Y. Calculation of molecular weight distribution from molecular weight moments in free radical polymerization. *Ind. Eng. Chem. Res.* **1997**, *36*, 1419−1423.
(13) Crowley, T. J.; Choi, K. Y. Optimal control of molecular weight distribution in a batch free radical polymerization process. *Ind. Eng. Chem. Res.* **1997**, *36*, 3676−3684.
(14) Crowley, T. J.; Choi, K. Y. Experimental studies on optimal molecular weight distribution control in a batch-free radical polymerization process. *Chem. Eng. Sci.* **1998**, *53*, 2769−2790.
(15) Chang, J. S.; Liao, P. H. Molecular weight control of a batch polymerization reactor: Experimental study. *Ind. Eng. Chem. Res.* **1999**, *38*, 144−153.
(16) Kiparissides, C.; Seferlis, P.; Mourikas, G.; Morris, A. J. Online optimizing control of molecular weight properties in batch free-radical polymerization reactors. *Ind. Eng. Chem. Res.* **2002**, *41*, 6120−6131.
(17) Alhamad, B.; Romagnoli, J. A.; Gomes, V. G. On-line multivariable predictive control of molar mass and particle size distributions in free-radical emulsion copolymerization. *Chem. Eng. Sci.* **2005**, *60*, 6596−6606.
(18) Park, M. J.; Rhee, H. K. Control of copolymer properties in a semibatch methyl methacrylate/methyl acrylate copolymerization reactor by using a learning-based nonlinear model predictive controller. *Ind. Eng. Chem. Res.* **2004**, *43*, 2736−2746.
(19) Wang, J. F.; Huang, H. Q.; Huang, X. Y. Molecular weight and the mark-houwink relation for ultra-high molecular weight charged polyacrylamide determined using automatic batch mode multi-angle light scattering. *J. Appl. Polym. Sci.* **2016**, *133*, DOI: 10.1002/app.43748.
(20) Bindlish, R. Nonlinear model predictive control of an industrial polymerization process. *Comput. Chem. Eng.* **2015**, *73*, 43−48.
(21) Maner, B. R.; Doyle, F. J.; Ogunnaike, B. A.; Pearson, R. K. Nonlinear model predictive control of a simulated multivariable polymerization reactor using second-order volterra models. *Automatica* **1996**, *32*, 1285−1301.
(22) Reed, W. F.; Alb, A. M. *Monitoring Polymerization Reactions: From Fundamentals to Applications*; Wiley: Hoboken, NJ, 2013.
(23) McAfee, T.; Leonardi, N.; Montgomery, R.; Siqueira, J.; Zekoski, T.; Drenski, M. F.; Reed, W. F. Automatic control of polymer molecular weight during synthesis. *Macromolecules* **2016**, *49*, 7170−7183.
(24) Ghadipasha, N.; Geraili, A.; Romagnoli, J. A.; Castor, C. A.; Drenski, M. F.; Reed, W. F. Combining on-line characterization tools with modern software environments for optimal operation of polymerization processes. *Processes* **2016**, *4*, 5.
(25) Schlegel, M.; Stockmann, K.; Binder, T.; Marquardt, W. Dynamic optimization using adaptive control vector parameterization. *Comput. Chem. Eng.* **2005**, *29*, 1731−1751.
(26) Alvarez, J. Output-feedback control of nonlinear plants. *AIChE J.* **1996**, *42*, 2540−2554.
(27) Bastin, G.; Dochain, D. *On-line Estimation and Adaptive Control of Bioreactors*; Elsevier: Amsterdam, 1990.
(28) Reed, W. Automated continuous online monitoring of polymerization reactions (acomp) and related techniques. In *Encyclopedia of Analytical Chemistry*, Meyers, R. A., Ed.; John Wiley & Sons, Ltd: Chichester, U.K., 2000; p 1.10.1002/9780470027318.a9288

DOI: 10.1021/acs.iecr.7b01074
Ind. Eng. Chem. Res. 2017, 56, 7322−7335